Negative-ion photodetachment in a weak magnetic field

Chris H. Greene
Department of Physics and Astronomy, Louisiana State University, Baton Rouge, Louisiana 70803
(Received 5 June 1987)

A sequence of three frame transformations is used to describe the escape of a photoelectron into a uniform magnetic field. Standard elements of quantum-defect theory are combined with a Harmin-Fano-type local frame transformation from spherical to cylindrical coordinates, accounting nonperturbatively for the electron motion in both the magnetic field and the field of the atom. A dramatic dependence of the cross section on the incident light polarization is predicted whenever s waves are not present at threshold, as in H^- photodetachment.

I. INTRODUCTION

Several years ago Blumberg, Jopson, and Larson[1] made the first observation of negative-ion photodetachment in the presence of a uniform magnetic field. At the field strengths used, $B \lesssim 10$ kG, the motion of electrons in the negative ion is hardly perturbed by such a weak field, but its effect on the photodetachment spectrum is dramatic nevertheless. The most conspicuous field effect is its modulation of the photodetachment continuum owing to the Landau quantization of the detached electron's motion across the magnetic field.

In order to interpret these measurements Blumberg, Itano, and Larson[2] (hereafter BIL) described the motion of the detached electron using the Landau-channel wave functions of a *free* electron in a magnetic field. This treatment, when combined with appropriate angular momentum weighting factors relevant to the particular negative ion studied (S^-), accounts for most of the initial observations. It also predicts, surprisingly, that the photodetachment cross section *diverges to infinity* at each Landau threshold, rising in proportion to $(E-E_{\rm th})^{-1/2}$. Clark showed later[3] that this divergence is an artifact deriving from the total neglect of electron-atom interactions in the final state. This paper pointed out that the usual Wigner threshold law $\sigma \propto (E-E_{\rm th})^{1/2}$ should in fact apply in the immediate vicinity of each threshold. A brute force R-matrix procedure outlined in Ref. 3 should, in principle, be capable of dealing simultaneously with the cylindrical (Landau) structure of the wave function at infinity and with the electron-atom interactions at smaller radii which are described most naturally in spherical coordinates. Such a calculation has not been performed, mainly because of the enormous number of Landau channels (typically of order 10^3 or larger) that are required for any such calculation to be realistic.

In this paper a theoretical treatment of this problem is developed which includes the electron-atom interaction and the electron-field interaction on an equal footing. Starting from an LS-coupled complex at small distances where the photon is absorbed, a sequence of three frame transformations is applied to the wave function as the photoelectron escapes. These are depicted schematically in Fig. 1. Within the reaction zone at $r \lesssim r_{LS\text{-}jj}$ the de Broglie phase of the electron is determined mainly by the total orbital L and spin S angular momenta of the final negative-ion continuum state. Somewhat further out, the exchange interaction has decayed exponentially to zero; here the electron wave function must instead be described by a jj-coupled channel expansion since the electron phase accumulates at a different rate $k_i=[2(E-E_{j_i})]^{1/2}$ depending on the residual atomic fine-structure state j_i. This LS-jj geometric frame transformation has been a standard element of previous quantum-defect analyses in many different contexts, including the study of zero-field detachment by Rau and Fano.[4]

The effect of the magnetic field has been totally neglected to this point, because the influence of laboratory strength fields is extremely weak compared to the scale of atomic forces at smaller radii. As the electron evolves to much larger radii, however, it begins to be affected profoundly by the field in two stages. First, at $r > r_{jj\text{-Zeeman}}$, the electron phase starts to vary depending on the specific Zeeman level in which the residual atom has been left, and depending also on the electron-spin

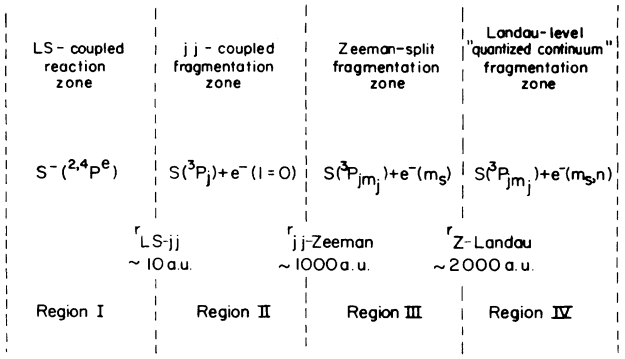

FIG. 1. Schematic illustration of the four regions involved in the escape of a photoelectron in the field of a neutral sulfur atom and of a uniform magnetic field. Distances shown are order-of-magnitude estimates, assuming a 5-kG magnetic field and an electron kinetic energy of 0.1 eV.

direction. A second frame transformation is therefore needed to describe the electron wave function by an expansion into Zeeman-split channels. This transformation, like the first, is accomplished using simple Wigner coefficients. In the last stage occurring at still larger radii, $r > r_{\text{Z-Landau}}$, the diagmagnetic term $\frac{1}{2}\alpha^2\rho^2$ in the Hamiltonian prevents the electron from escaping in any direction except parallel to the field axis. Qualitatively, the spherical outgoing wave function of the photoelectron is diabatically projected onto the energetically accessible, cylindrical Landau channels. The description of this last step in the outward propagation of the electron wave function utilizes a local, nonunitary frame transformation of the type developed by Harmin[5] and Fano.[6] In that context, the small-r spherical wave function evolves into a channel expansion in parabolic coordinates. Here the same idea is used in the sense that the field effect is expressed finally as a density-of-states matrix, but the nature of the spherical-to-cylindrical transformation is considerably different.

The Harmin-Fano local frame transformation method also seems ripe for extension to other problems which are separable in different coordinate systems in two distinct regions of configuration space. Another article[7] develops a similar analysis to treat negative-ion photodetachment in an electric field. This theoretical technique might have relevance even to the quasi-Landau problem of an atomic Rydberg electron affected by a uniform magnetic field, for which current theoretical descriptions are not satisfactory.[8] This will require a nontrivial generalization of the current approach, however, since the large-r Schrödinger equation for the electron in a Coulomb and diagmagnetic potential is not separable in any coordinate system. Nevertheless, the quasi-Landau Hamiltonian is approximately separable in spherical coordinates near the nucleus and in cylindrical coordinates at large distances.

The paper will be organized as follows. Section II develops the required theoretical analysis associated with the sequence of orthogonal and nonorthogonal frame transformations. The analysis is applied to S^- photodetachment in a 6-kG field, which is essentially a one-electron problem in the energy range considered. A second example considered in Sec. III is the photodetachment of Rb^- in a magnetic field, which shows a more complicated effect in the vicinity of a doubly excited negative-ion resonance near the $Rb(5p_{1/2})$ threshold. A discussion of the theoretical method and its limitations follows in Sec. IV.

II. THE THREE-STEP FRAME TRANSFORMATION FOR S^- PHOTODETACHMENT

As a photoelectron escapes from a residual sulfur atom, it encounters four distinct regions depicted in Fig. 1. Three frame transformations are therefore needed to "propagate" the small-r wave function outward to infinity. Electron motion through the first three regions is separable in spherical coordinates, and accordingly the first two transformations are orthogonal as usual. These are discussed in Sec. II A below. The frame transformation from region III into region IV is nonorthogonal, however, owing to the cylindrical separation required in region IV. Its implementation involves several new elements and is described separately in Sec. II B. Details of the application of this treatment to S^- detachment are presented in Sec. II C.

A. Orthogonal frame transformations by angular momentum recouplings

At small radii, $r \lesssim 10$ a.u., the electron remains within the range of the atomic electrons, and the atom-electron interactions are strong. In particular, the exchange interaction overwhelms all fine-structure terms in the Hamiltonian and all magnetic terms as well. The eigenstates of the system within region I must therefore be LS coupled. This includes the entire localized initial state of S^-, $p^5\,{}^2P^0_{3/2}$ and also the part of the final continuum state within region I, which must be $p^4s\,{}^2P^e$ since dipole absorption does not affect the total spin directly. This doublet spin state ($S=\frac{1}{2}$) will in fact become coupled to the quartet state ($S=\frac{3}{2}$)$p^4s\,{}^4P^e$, owing to boundary conditions to be imposed beyond region I, at $r > r_{LS\text{-}jj}$. In any case the relevant scattering parameters needed to describe the region-I final state are a doublet and a quartet scattering length a_d, a_q. Their values, which Rau and Fano[4] obtained by semiempirically fitting zero-field detachment cross sections, represent the starting point for our analysis,

$$a_d = 3.5, \quad a_q = -10 \ . \tag{1}$$

If there were (a) no fine-structure splitting in the sulfur ground state, and (b) no external magnetic field, then region I would extend to infinity and its (smooth, analytic) reaction matrix would be diagonal,

$$K^{(0,\mathrm{I})}_{S,S'} = -a_S \delta_{SS'} \ . \tag{2}$$

That is, for each alternative spin coupling, the wave function of an escaping electron would have the $r \gtrsim 10$ a.u. form (aside from normalization),

$$F^{(\mathrm{I})}_S(r) = f^0(r) + g^0(r) a_S \ , \tag{3}$$

for $S=\frac{1}{2},\frac{3}{2}$. Here $f^0=(2/\pi k^2)^{1/2}\sin(kr)$ and $g^0=-(2/\pi)^{1/2}\cos(kr)$ are regular and irregular s-wave radial solutions, respectively, analytic in the energy, as described in Refs. 4 and 9–11. Because $K^{(0,\mathrm{I})}_{S,S'}$ is smooth, it can even be regarded as energy independent over the range considered in this paper.

In fact the ground state of sulfur is split into three fine-structure levels ^3P_j with $j=2,1,0$. The first frame transformation, from region I into region II, accounts for this complication by noting that each alternative arrangement $S(j)+e^-$ represents a different fragmentation channel. Clearly the electronic wave vector at infinity k_j depends on this quantum number j. The region-II wave function is accordingly characterized by a nondiagonal (analytic in E, smooth) reaction matrix $K^{(0,\mathrm{II})}_{jj'}$, for each total angular momentum J and component M_J,

$$\Psi^{(\mathrm{II})}_{j'} = \mathcal{A} \sum_j \phi^{(JM_J)}_j [f^0_j(r)\delta_{jj'} - g^0_j(r) K^{(0,\mathrm{II})}_{jj'}(J)] \ . \tag{4}$$

Here $\mathcal{A}$ denotes antisymmetrization while $\phi_j^{(JM_J)}$ contains the wave function of ^3P_j sulfur and the spin and orbital degrees of freedom of the photoelectron, all coupled to form a total J,M_J. The frame transformation theory[4,9–11] derives $K_{jj'}^{(0,\mathrm{II})}(J)$ in terms of the a_S by introducing the orthogonal recoupling matrix element,[12]

$$V_{jS}^{(J)}=((L_aS_a)js_e \mid L_a(S_as_e)S)^{(J)} . \tag{5}$$

In Eq. (5) $L_a=1$ and $S_a=1$ are the orbital and spin angular momenta of ground-state sulfur, $s_e=\frac{1}{2}$ is the photoelectron spin, S is the total spin of the final state S^-, and j is the total angular momentum of the atomic residue. The region-II reaction matrix is then independent of M_j,

$$K_{jj'}^{(0,\mathrm{II})}(J)=-\sum_S V_{jS}^{(J)}a_S V_{j'S}^{(J)} . \tag{6}$$

Considering photodetachment from an initial $J_0=\frac{3}{2}$ state, the final-state angular momenta are $J=\frac{1}{2},\frac{3}{2},\frac{5}{2}$. Close to the lowest threshold ($j=2$), however only $J=\frac{3}{2}$ and $\frac{5}{2}$ contribute since $\mathbf{J}=\mathbf{j}+\mathbf{s}_e$ must be satisfied. Two channels ($j=1,2$) are therefore involved for $J=\frac{3}{2}$, while only $j=2$ contributes to the $J=\frac{5}{2}$ final state. In the case of $J=\frac{3}{2}$, the closed $j=1$ channel must be "eliminated" in the sense of quantum defect theory (QDT),[10] by forcing its wave-function component to vanish at infinity. This elimination replaces the $J=\frac{3}{2}$ reaction matrix by a single phase shift,

$$\tan\delta_{J=3/2}^{(0,\mathrm{II})}=K_{22}^{(0,\mathrm{II})}-[K_{12}^{(0,\mathrm{II})}]^2\kappa_1/[1+\kappa_1K_{11}^{(0,\mathrm{II})}] . \tag{7}$$

In terms of the atomic sulfur energy levels E_j, $\kappa_j=[2(E_j-E)]^{1/2}$. The corresponding eigenphaseshift for $J=\frac{5}{2}$ is given in terms of the quartet scattering length by

$$\tan\delta_{J=5/2}^{(0,\mathrm{II})}=-a_q . \tag{8}$$

As the detached electron propagates outward to the vicinity of $r_{jj\text{-Zeeman}}$, the phase kr of its wave function begins to differ depending on the combined Zeeman sublevel of the sulfur atom $S(jm_j)$ and the photoelectron spin $e^-(s_em_e)$. This Zeeman sublevel structure for the final state takes the form, for $j=2$,

$$E_{jm_jm_e}=E_j+\alpha(g_fm_j+2m_e) \tag{9}$$

in terms of the magnetic field parameter,

$$\alpha=B/(4.69\times10^9\ \mathrm{G}) , \tag{10}$$

which is half the cyclotron frequency in atomic units. The final atomic state ($j=2$) and initial ion state ($J_0=\frac{3}{2}$) gyromagnetic ratios are

$$g_f=\tfrac{3}{2},\quad g_0=\tfrac{4}{3} , \tag{11}$$

and the initial state of S^- has Zeeman sublevels $E_{J_0M_0}=E_{J_0}+\alpha g_0M_0$. With the magnetic field nonzero, J is no longer a good quantum number for the final continuum state, and the cross-section calculation must be performed separately for each (M_0,M_J). The next frame transformation from $|JM_J)$ to $|jm_j,s_em_e)$ is accomplished by the Clebsch-Gordan coefficients

$$X_{m_jm_e,J}^{(M_J)}=(jm_j,s_em_e \mid JM_J) . \tag{12}$$

The region-III (analytic) reaction matrix becomes

$$K_{m_jm_e,m_j'm_e'}^{(0,\mathrm{III})}(M_J)=\sum_J X_{m_jm_e,J}^{(M_J)}\tan\delta_J^{(0,\mathrm{II})}X_{m_j'm_e',J}^{(M_J)} . \tag{13}$$

The calculation of cross sections now utilizes the reaction matrix $\underline{K}^{(\mathrm{III})}$ in a base set of energy-normalized comparison functions (f_i,g_i). The general connection to (f_i^0,g_i^0) usually involves parameters A_i and $\mathcal{G}_i$ characteristic of the long-range potential in the relevant channel $i=(m_j,m_e)$. For an s wave in zero field, appropriate here throughout region III, $\mathcal{G}_i=0$ and A_i is simply $k_i^{1/2}=[2(E-E_{jm_jm_e})]^{1/4}$ if the final-state total energy is E. Then $f_i=k_i^{1/2}f_i^0$ and $g_i=k_i^{-1/2}g_i^0$ and the energy-normalized reaction matrix is

$$K_{ii'}^{(\mathrm{III})}(M_J)=k_i^{1/2}K_{ii'}^{(0,\mathrm{III})}(M_J)k_{i'}^{1/2} . \tag{14}$$

[If any of the k_i are imaginary for a specific final-state energy E, then the ith channel must also be eliminated by a generalization of Eq. (7). The expression required is Eq. (11) of Ref. 13, except that $\tan\beta$ must be replaced by κ^{-1}.] Thus the final matrix $K^{(\mathrm{III})}$ has indices associated with open channels only. The eigenvalues of this reaction matrix will be denoted $\tan\delta_\rho$ and the orthonormal eigenvectors $T_{i\rho}$, so that

$$K_{ii'}^{(\mathrm{III})}=\sum_\rho T_{i\rho}\tan\delta_\rho(\tilde{T})_{\rho i'} . \tag{15}$$

Our calculation requires also the dipole matrix elements connecting the ground state to our final state $\psi_\rho^{(M_J)}$, which can be obtained by a linear transformation from the "analytic" eigenchannels characterized by J to the "energy-normalized" eigenchannels characterized by ρ. First of all, the Wigner-Eckart theorem isolates the M_J dependence of the "J" matrix elements,

$$\begin{aligned} d_J^{(0,M_J)}&=(\psi_{JM_J}^{(0,\mathrm{II})} \mid \boldsymbol{\epsilon}\cdot\mathbf{r} \mid \psi_{J_0M_0}) \\ &=[(J\|r^{(1)}\|J_0)/(2J+1)^{1/2}](JM_J \mid J_0M_0,1q) . \end{aligned} \tag{16}$$

We will abbreviate the quantity in square brackets $[\cdots]$ by D_J, and note that it is nonzero for $J=\frac{3}{2}$, while it vanishes for $J=\frac{5}{2}$ since the latter requires the total electronic spin to be $S=\frac{3}{2}$ in the final state. We will also regard $D_{3/2}$ to be essentially constant over the energy range considered, within a few cm^{-1} of the $j=2$ threshold(s). (If desired over a larger energy range, its energy dependence could be found in terms of a region-I reduced dipole matrix element as discussed by Rau and Fano.[4]) The final transformation to the energy-normalized matrix element is now given by Eqs. (3.4) and (3.5) of Ref. 14,

$$\begin{aligned} d_\rho^{(M_J)}&=D_{3/2}\frac{(\frac{3}{2}M_J \mid J_0M_0,1q)}{\cos\delta_{3/2}^{(0,\mathrm{II})}} \\ &\times\sum_{m_j,m_e}X_{m_jm_e,J=3/2}^{(M_J)}k_{m_jm_e}^{1/2}T_{m_jm_e,\rho}\cos\delta_\rho . \end{aligned} \tag{17}$$

B. The transformation from spherical to cylindrical coordinates

At this point we have only accounted for the linear Zeeman term in the magnetic field Hamiltonian. The term quadratic in B becomes important only at electronic distances approaching 10^3 bohr radii, but its effect on the spectrum is dramatic, quantizing the motion orthogonal to the magnetic field and permitting escape to infinity along the field axis only. Asymptotically the field imposes a cylindrical symmetry on the system, in contrast to the spherically symmetric escape of the photoelectron through regions I–III. On the other hand, the electron is a free particle throughout most of its motion, which permits separation of its wave equation in *either* spherical or cylindrical coordinates. This fact permits us to account for the asymptotic cylindrical symmetry by a third frame transformation which will describe the manner in which a spherical outgoing wave projects itself among the assorted Landau channels which are available. Unlike the preceding two transformations which produced the region-III wave function, however, this involves a *local, nonorthogonal frame transformation* very similar to the transformation theory developed by Harmin[5] to describe the nonhydrogenic Stark effect.

Equation (17) is a dipole matrix element connecting the ground state to a final-state collision eigenchannel having the following form in region III:

$$\Psi_\rho = \mathcal{A} r^{-1} \sum_i \phi_i(\omega)[f_i(r)T_{i\rho}\cos\delta_\rho - g_i(r)T_{i\rho}\sin\delta_\rho] \ . \tag{18}$$

Here the number of independent solutions Ψ_ρ equals the number of open channels at a given E and M_J, which is in turn equal to the number of indices i. The evolution of this wave function through region IV to infinity requires a local frame transformation[5,6] between the regular, energy-normalized solutions appropriate in the small-r (spherical) and large-r (cylindrical) regimes. The regular spherical solutions in zero field are the familiar

$$f_{lm}(\mathbf{r}) = (2\pi)^{-1/2} N_{lm} e^{im\phi} P_{lm}(\cos\theta)(2k/\pi)^{1/2} j_l(kr) \ . \tag{19}$$

The regular cylindrical solutions in zero field have different forms depending on the parity in z, $\pi_z = \pi_{\rm tot}(-1)^m$, and as usual $\pi_{\rm tot} = (-1)^l$ is the total parity:

$$\psi^{B=0}_{qm}(\mathbf{r}) = (2\pi)^{-1/2} e^{im\phi} J_m[(k^2 - q^2)^{1/2}\rho] \times (\pi q)^{-1/2} \times \begin{cases} \cos(qz), & \pi_z = +1 \\ \sin(qz), & \pi_z = -1. \end{cases} \tag{20}$$

The z component of the electron wave vector is q, which ranges from 0 to k. The complementary sets of separable solutions (19) and (20) are interrelated by a transformation matrix $\underline{U}$ which can be extracted from an integral tabulated in Ref. 15,

$$\psi^{B=0}_{qm}(\mathbf{r}) = \sum_l U^{B=0}_{ql}(m) f_{lm}(\mathbf{r}) \ , \tag{21}$$

where

$$U^{B=0}_{ql}(m) = \left[\frac{2l+1}{kq}\right]^{1/2} \left[\frac{(l-m)!}{(l+m)!}\right]^{1/2} \times (-1)^{[(l-1-m)/2]} P_{lm}(q/k) \ . \tag{22}$$

In the phase factor $(-1)^{[x]}$ here, $[x]$ denotes the smallest integer greater than or equal to x. The summation in (21) should include only the even or else only the odd values of l, depending on $\pi_{\rm tot}$. This transformation is an orthogonal one in the sense that

$$f_{lm}(\mathbf{r}) = \int_0^{k^2/2} d(\tfrac{1}{2}q^2) \psi^{B=0}_{qm}(\mathbf{r}) U^{B=0}_{ql}(m) \ . \tag{23}$$

The generalization of this transformation to nonzero magnetic fields closely follows the Stark treatment of Ref. 5. To begin with, the exact cylindrical solutions in the presence of a magnetic field B generating a cyclotron frequency 2α are well known,

$$\psi^B_{nm}(\mathbf{r}) = (2\pi)^{-1/2} e^{im\phi} N_{nm} e^{-\alpha\rho^2/2} (\alpha\rho^2)^{|m|/2} L_n^{(|m|)}(\alpha\rho^2)(\pi q_n)^{-1/2} \times \begin{cases} \cos(q_n z), & \pi_z = +1 \\ \sin(q_n z), & \pi_z = -1. \end{cases} \tag{24}$$

The normalization coefficient is[16]

$$N_{nm} = [2\alpha n!/(n+|m|)!]^{1/2} \ . \tag{25}$$

The values of the momentum q_n along the field axis which are allowed at any energy $\frac{1}{2}k^2$ are now quantized because of the Landau-level structure in the continuum,

$$\tfrac{1}{2}k^2 = E_n^{(m)} + \tfrac{1}{2}q_n^2 \equiv \alpha(2n + m + |m| + 1) + \tfrac{1}{2}q_n^2 \ . \tag{26}$$

The key consideration needed here is the fact that for the typically weak fields available in the laboratory, the diamagnetic term $\frac{1}{2}\alpha^2\rho^2$ in the Hamiltonian is negligible at small distances. Consequently the $B=0$ and the $B\neq 0$ solutions must be proportional there, to a very good approximation. Multiplying the zero-field result (22) by this proportionality factor and by the factor 2α needed to convert integrals over $d(\frac{1}{2}q^2)$ into summations over n, we obtain the transformation coefficient,

$$U_{nl}(m) = U^{B=0}_{q_n l}(m)(2\alpha)^{1/2}[n!/(n+|m|)!]^{1/2} \times [\tfrac{1}{2}(2n + m + |m| + 1)]^{|m|/2} \ . \tag{27}$$

This matrix element relates the spherical and cylindrical solutions (at small $r \ll \alpha^{-1/2}$ only),

$$\psi^B_{nm}(\mathbf{r}) = \sum_l U_{nl}(m) f_{lm}(\mathbf{r}) \ . \tag{28}$$

A key element emphasized in Ref. 5 is that the matrix $\underline{U}$ is not orthogonal for $B \neq 0$, so that the inverse transformation will just be written formally as

$$f_{lm}(\mathbf{r}) = \sum_{n=0}^{n_{\max}} (\underline{U}^{-1})_{ln} \psi^B_{nm}(\mathbf{r}) \ . \tag{29}$$

The summation over n includes all Landau levels for which $E_n^{(m)} < \frac{1}{2}k^2$. The nonorthogonality of $\underline{U}$ arises because ψ^B_{nm} and f_{lm} do not satisfy the same Schrödinger equation everywhere, in particular at large distances. Accordingly these transformations are only valid *locally*, unlike the zero-field result (21) which holds everywhere.

The same matrix $\underline{U}$ also allows us to relate the solutions irregular at $r=0$, because the cylindrical and spherical principal part Green's functions must coincide.[6] The irregular spherical solution $g_{lm}(\mathbf{r})$, which lags $f_{lm}(\mathbf{r})$ by 90° at large r, is given by Eq. (19) with $j_l(kr)$ replaced by $n_l(kr)$. Similarly the irregular cylindrical solution $\chi^B_{nm}(\mathbf{r})$ which lags $\psi^B_{nm}(\mathbf{r})$ by 90° in z, is given by Eq. (24) with $\cos(qz)$ replaced by $\sin(qz)$ for $\pi_z = +1$ and $\sin(qz)$ replaced by $-\cos(qz)$ for $\pi_z = -1$. Since there is no potential barrier between $z=0$ and $|z| \to \infty$, the parameter $\csc\gamma$ in Eq. (50) of Ref. 5 reduces to unity for the present problem. This reflects the ability of $\sin(qz)$ and $\cos(qz)$ to maintain their 90° phase difference at both small and large $|z|$, unlike the parabolic continuum functions of Ref. 5. The relationship between these irregular solutions can then be expressed as

$$\chi^B_{nm}(\mathbf{r}) = \sum_l (\tilde{U})^{-1}_{nl} g_{lm}(\mathbf{r}) \ , \tag{30a}$$

$$g_{lm}(\mathbf{r}) = \sum_{n=0}^{n_{\max}} (\tilde{U})_{ln} \chi^B_{nm}(\mathbf{r}) \ . \tag{30b}$$

The region-III solution ψ_ρ thus evolves into a region-IV solution of the form

$$\psi_\rho = A \sum_{i,n} \phi_i T_{i\rho} [\psi^B_{nm_i}(\mathbf{r}) \cos\delta_\rho (U^{-1})_{l_i n} - \chi^B_{nm_i}(\mathbf{r}) \sin\delta_\rho (\tilde{U})_{l_i n}] \ . \tag{31}$$

The quantum numbers l_i and m_i are in fact zero here close to the detachment threshold, owing to the dominance of s waves at threshold, though we leave them explicitly in Eq. (31) for generality. Note also that the matrix $\underline{U}$ depends on the i index through its wave vector k_i in addition to l_i. Calculation of the overlap matrix $\langle \psi_\rho | \psi_{\rho'} \rangle$ as in Ref. 5 leads to the density-of-states matrix for a multichannel problem,

$$D^B_{\rho\rho'} = [\langle \Psi | \Psi' \rangle^{-1}]_{\rho\rho'} \ , \tag{32}$$

where

$$\langle \Psi_\rho | \Psi_{\rho'} \rangle = \sum_i [\cos\delta_\rho \tilde{T}_{\rho i} H_i^{-1} T_{i\rho'} \cos\delta_{\rho'} + \sin\delta_\rho \tilde{T}_{\rho i} H_i T_{i\rho'} \sin\delta_{\rho'}] \ , \tag{33}$$

and with the field effects contained in the "modulating factor,"

$$H_i = \sum_{n=0}^{n_{\max}} (\tilde{U})_{l_i n} U_{n l_i} = \sum_n (U_{n l_i})^2 \ . \tag{34}$$

The total photodetachment cross section is then simply

$$\sigma^B = (4\pi^2\omega/137) \sum_{\rho,\rho'} d_\rho D^B_{\rho\rho'} d_{\rho'} \ . \tag{35}$$

The matrix inversion of $\langle \Psi | \Psi' \rangle$ in Eq. (32) is of dimension 2×2 for each M_J, while the H_i and H_i^{-1} are in fact scalars here.

Figure 2 shows the single channel modulating factor H for a 10.7-kG magnetic field, for three different partial waves. In the experiments performed to data, a near-threshold electron is ejected predominantly into the $l=0$ partial wave owing to the Wigner threshold law. In this case the magnetic field is seen [Fig. 2(a)] to induce a quasiperiodic modulation of the photoelectron density of states, oscillating about the mean value $H=1$. Note that, whereas the factor H diverges at each Landau threshold, the relevant element of the density-of-states

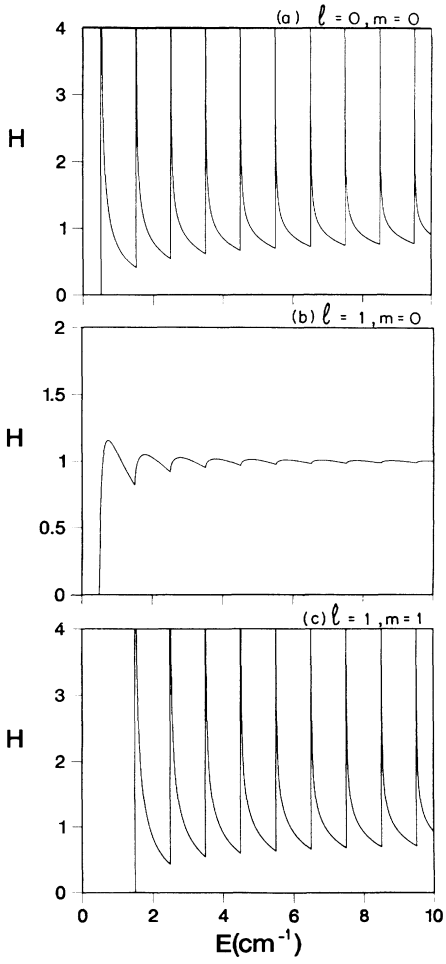

FIG. 2. Dimensionless modulating factor for a 10.7-kG magnetic field, containing the main effect of the external field on the photoelectron density of states. Three partial waves are shown: (a) $(lm)=(00)$, (b) $(lm)=(10)$, (c) $(lm)=(11)$.

matrix D^B approaches in that limit a constant plus a term rising in proportion to the usual Wigner threshold factor $(E\text{-}E_{\rm th})^{1/2}$. This agrees with Clark's analysis.[3] But if all eigenphase shifts vanish identically, corresponding to no electron-atom interaction, then D^B diverges at each threshold as expected from BIL.[2] See also Refs. 17 and 18 for further discussion of this point. This last limit is nearly realized very close to a (zero-field) detachment threshold, where again the eigenphase shifts are small because of the Wigner threshold factor. In this energy range the BIL treatment is thus reasonably sound.

Figures 2(b) and 2(c) show that when an $l=1$ photoelectron is ejected, as in H^-, the density of states depends very strongly on the light polarization $\hat{\epsilon}$. For $l=1$, $m=0$ ($\hat{\epsilon}$ parallel to **B**), the strong modulation of the cross section practically disappears. This makes sense physically because the photoelectron is ejected mainly along the field in a $\cos^2\theta$ distribution, and is unlikely to range outward to large ρ values. Consequently a negligible amount of electron flux is projected into the highest, newly opening Landau channel near that Landau threshold. For $l=1$, $m=1$, on the other hand ($\hat{\epsilon}$ perpendicular to **B**), the modulations are somewhat stronger than for s waves because the electron is preferentially ejected at right angles to the field and is much more likely to emerge in the highest accessible Landau channel.

C. Results for S^- Photodetachment

Figure 3 shows the predictions of Secs. II A and II B for the S^- detachment cross section in the presence of a 6-kG magnetic field. The incident light is taken here to be linearly polarized along the field axis. The spectrum displays many of the same features shown by BIL.[2] First of all, the $(E-E_{\rm th})^{-1/2}$ behavior is seen to dominate the visual appearance of the spectrum close to each Landau threshold $E_{\rm th}$, even though this divergent behavior does not apply all the way down to threshold. As discussed in Sec. II B, the usual Wigner behavior $(E-E_{\rm th})^{1/2}$ applies in the immediate vicinity of each threshold. In the example of Fig. 3, however, the energy range over which the Wigner law holds is extremely small, approximately 10^{-5} cm^{-1}. The analysis of BIL (Ref. 2) is apparently satisfactory here, a result of the fact that the zero-field scattering phase shifts are themselves extremely small in this near-threshold energy region. In fact, the threshold peaks shown are not consistently given to their actual height, since in most cases the peak heights would dwarf the scale shown. The *relative* strength of successive threshold peaks is correctly depicted, nevertheless. The dominance of a single pair of degenerate Zeeman transitions [$M_0=\pm\frac{3}{2}$ to $(m_j,m_e)=(\pm 2,\mp\frac{1}{2})$] follows from simple angular momentum coupling factors, as is clear from Fig. 3 of BIL.

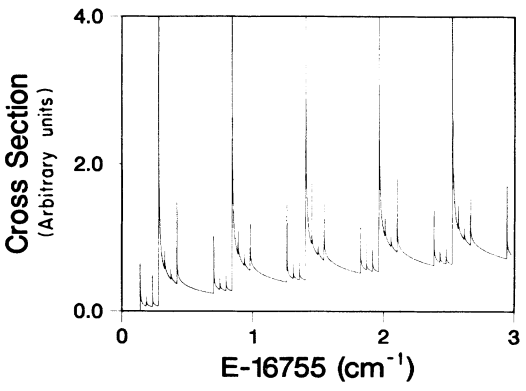

FIG. 3. Predicted photodetachment cross section for S^- ground-state ions in a 6-kG magnetic field. The incident light is assumed to be polarized linearly along the field axis.

An obvious conclusion from these results is that ignoring the zero-field electron-atom interaction [as done by BIL (Ref. 2)] is a good approximation close to any zero-field detachment threshold. That approach should fail, however, if a zero-field shape resonance lies just above threshold, or in the vicinity of any prominent resonance features. In these situations and those for which s waves are excluded by symmetry close to threshold, the approach of Secs. II A and II B should prove to be more generally applicable.

III. TREATMENT OF Rb^- PHOTODETACHMENT

The preceding results have demonstrated that quantum-defect theory successfully describes negative-ion photodetachment in a weak magnetic field. I turn now to a more complicated situation in which the negative ion possesses doubly excited autodetaching resonances. Extension of the Sec. II B local frame transformation to closed channels is nontrivial and will not be faced here. However, most resonances are localized at comparatively small radii and accordingly their "closed-channel" component is hardly affected by the weak magnetic field. At this level the only effect of the resonance is to induce a strong energy dependence in the phase shift of the continuum wave functions. Beyond this, no substantial modification of the Sec. II treatment is required.

As an application consider Rb^- photodetachment near the first excited thresholds $5p_{1/2,3/2}$ of Rb. Here the enormous static polarizability of Rb ($5p$) ($\alpha_{5p}\simeq 840$ a.u.) plays a crucial role, in contrast to the S^- example of Sec. II. In particular, this long-range polarization field causes a strong energy dependence of the zero-field reaction matrix $\underline{K}^0$, quite distinct from resonance effects. The cleanest theoretical method for incorporating this strong energy dependence into the formulation follows Ref. 19, which utilizes a reaction matrix relative to two independent (Mathieu function) solutions (f^p,g^p) of the Schrödinger equation in a polarization field. In this "generalized quantum defect" representation the reaction matrix varies more smoothly with energy than in the "zero-field" representation.

The zero-field photodetachment spectrum of Rb^- has been studied in detail in two high-resolution experiments by Rouze and Geballe[20] and by Frey *et al.*[21] Reference

20 in particular has fitted the polarization-based QDT (Ref. 19) to the spectrum and extracted the reaction matrix $\underline{K}^0$ near the $^2P_{1/2}$ and $^2P_{3/2}$ thresholds. Since they found that a single fit with energy-independent parameters is insufficient to reproduce the fine details at both thresholds, they tabulated slightly different parameters at each threshold. This energy dependence complicates our analysis somewhat, although it is not that surprising in the case of Rb^- since the splitting of the fine-structure levels of Rb($5p$) is over 200 cm^{-1}. To test whether the fits of Rouze and Geballe are sensible, we first calculate the photodetachment spectrum which is predicted by a linear interpolation between the parameters they tabulated at the two thresholds. [In fact the eigenquantum defects $\pi\mu_\alpha$ were interpolated rather than the $\tan(\pi\mu_\alpha)$ given in Ref. 20.] As shown in Figs. 4 and 5, the spectrum predicted by this interpolation reproduces the data well throughout this energy range, both the total cross section and the branching ratios. Accordingly this zero-field MQDT fit seems reliable, and we will use these interpolated parameters to predict the detachment spectrum in the presence of a magnetic field.

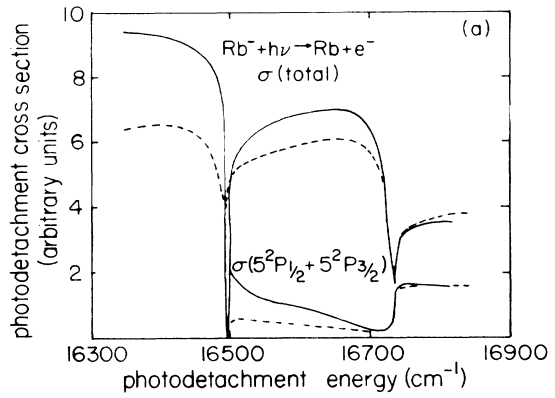

FIG. 4. Zero-field cross sections for Rb^- photodetachment near the Rb($5p$) fine-structure thresholds: (a) The smooth curves are the experimental total and partial cross sections of Frey *et al.* (Ref. 21), while the dashed curve is an MQDT fit by Rouze and Geballe (Ref. 20) at the $5p_{3/2}$ threshold. [From Rouze and Geballe (Ref. 20).] (b) Present calculated MQDT spectrum predicted using a linear interpolation between the parameters fitted by Ref. 20.

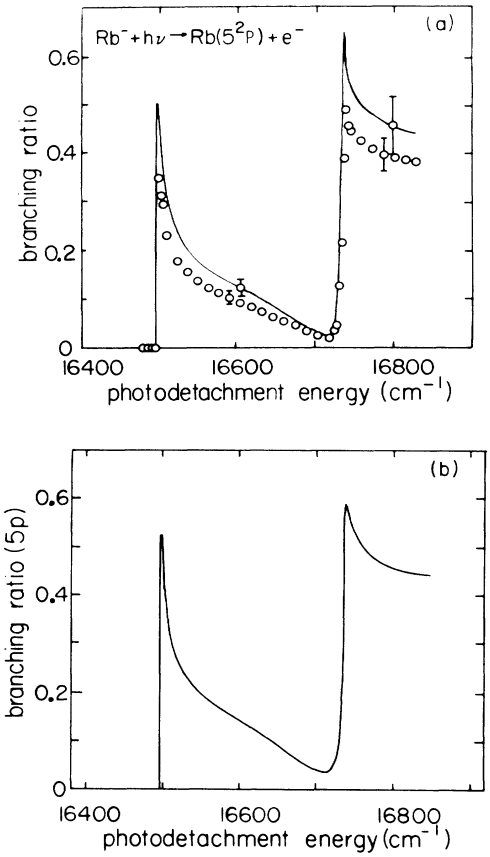

FIG. 5. Branching ratio $\sigma(5p)/\sigma(\text{total})$ is shown for Rb^- photodetachment in zero external field. (a) Experimental results of Rouze and Geballe (Ref. 20) (open circles) and of Frey *et al.* (Ref. 21) (smooth curve) [from Rouze and Geballe (Ref. 20).] (b) Present results using polarization MQDT, with linear interpolation of parameters fitted by Ref. 20.

The parameters which characterize the small-r solution (region I) are a 2×2 reaction matrix $K^{(0,I)}_{\bar\alpha,\bar\alpha'}$ for the $^1P^o$ final state and another for the $^3P^o$ final state. The channel labels on these matrices are $5s\epsilon p$ for $\bar\alpha=1$, $5p\epsilon s$ for $\bar\alpha=2$. Since we will ultimately be interested in the separate Zeeman-split channels we will regard the region-I reaction matrix (for $q=0$) as a single 8×8 reaction matrix,

$$\langle \bar\alpha, SM_S LM_L \mid K^{(0,I)} \mid \bar\alpha', S'M'_S LM'_L \rangle$$

which is block diagonal in S and M_S. Here only $L=1$ is allowed, and $M_S+M_L=q=M'_S+M'_L$ is a consequence of angular momentum conservation. Rather than going first to a jj-coupled region II (as done in Sec. II for S^-), it is simpler here to make a single frame transformation into the Zeeman-structured region III. The i fragmentation channels of region III are of a different nature for $5s\epsilon p$ and $5p\epsilon s$. For $5s\epsilon p$, ignoring the spin-orbit interaction for the outer p electron, the Zeeman channel structure looks like

$$\text{Rb}(5s_{1/2}, m_{s_a}) + e^-(s_e=\tfrac{1}{2}, m_{s_e}; L=1, M_L)\ , \qquad (36)$$

subject only to $m_{s_a}+m_{s_e}+M_L=M_J=q$. Thus $i=\{m_{s_a}, m_{s_e}, M_L\}$ for $5s\epsilon p$. For $5p\epsilon s$ the structure is different because of the atomic spin-orbit splitting, namely,

$$\mathrm{Rb}(5p\ ^2P_{jm_j})+e^-(s_e=\tfrac{1}{2},m_e;l_e=0)\ , \tag{37}$$

whereby $i=\{jm_j,m_e\}$ for all $5p\epsilon s$. channels. The transformation coefficient $X_{i\bar{\alpha}}$ can be derived using straightforward angular momentum algebra, giving

$$X_{i\bar{\alpha}}=\langle \tfrac{1}{2}m_{s_e},\tfrac{1}{2}m_{s_a} \mid SM_S\rangle \tag{38}$$

for the $5s\epsilon p$ channels ($i=1-4,\bar{\alpha}=$odd), and

$$X_{i\bar{\alpha}}=\sum_J \langle s_e m_e, jm_j \mid JM_J\rangle \times\langle s_e(s_aL)j \mid (s_es_a)SL\rangle^{(J)}\langle JM_J \mid SM_S,LM_L\rangle \tag{39}$$

for $5p\epsilon s$ ($i=5-8,\bar{\alpha}=$even). Then the region-III analytic reaction matrix is

$$K_{ii'}^{(0,\mathrm{III})}=\sum_{\bar{\alpha},\bar{\alpha}'} X_{i\bar{\alpha}}K_{\bar{\alpha},\bar{\alpha}'}^{(0,\mathrm{I})}(\tilde{X})_{\bar{\alpha}'i'}\ . \tag{40}$$

The transformation to an energy-normalized reaction matrix $K^{(\mathrm{III})}$ now involves parameters A_i and $\mathcal{G}_i$ for the polarization potential as tabulated for s electrons in Ref. 19. [As in Ref. 19, the polarization solutions were not actually used to describe the p electron in the $5s\epsilon p$ channel since the $5s$ polarizability induces no rapid variations with energy close to Rb(5p).] At each energy now the N_c closed channels are "eliminated" to give an $N_0\times N_0$ open-channel K matrix which can be diagonalized to yield the δ_ρ and $T_{i\rho}$ of Sec. II. Similarly, the $^1P^o$ dipole matrix elements in region I can be transformed to give the desired d_ρ. Now the last frame transformation into region IV is accomplished, defining the density-of-states matrix through Eqs. (32) and (33). Equation (35) at last produces the total photodetachment cross section, as shown in the figures near the $^2P_{1/2}$ threshold.

Figure 6 shows the resulting spectrum of Rb^- predicted by this analysis. Note that a major influence of the magnetic field is its Zeeman splitting of the $j=\frac{1}{2}$ channels of $\mathrm{Rb}+e^-$, which divides the narrow window resonance below threshold into two resonances. The Landau substructure is also significant, but above the Rb($5p$) threshold only. In fact, some Landau structure associated with the $5s\epsilon p$ continuum is present just below the $5p_{1/2}$ threshold also, but it is extremely weak for the present case with the incident light polarized linearly along the field axis, as this leads predominantly to the $l=1$, $m_l=0$ partial wave for the photoelectron [see Fig. 2(b).] The continuum Landau structure just below Rb($5p$) becomes much more visible, on the other hand, if the incident radiation is circularly polarized along the magnetic field.

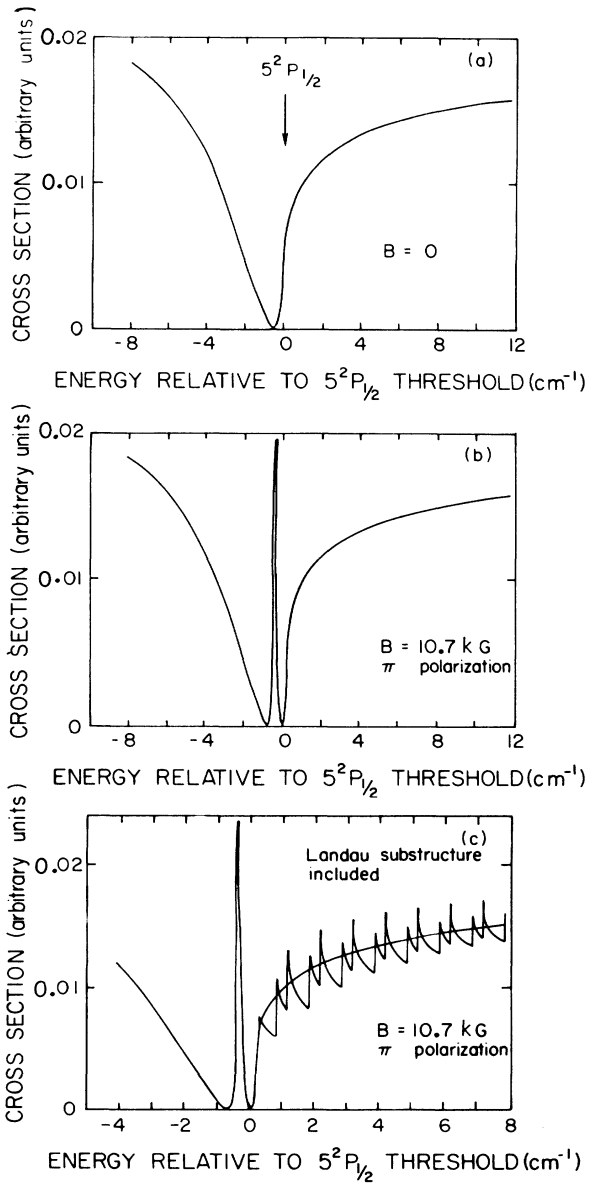

FIG. 6. Predicted Rb^- photodetachment cross section near the $5p_{1/2}$ threshold with (a) the magnetic field absent, (b) only the linear Zeeman effect of the field included, and (c) the full field effect included. The field strength used in (b) and (c) is 10.7 kG and the incident light is taken to be linearly polarized along the magnetic field axis.

IV. LIMITATIONS OF THE FORMULATION

In Harmin's treatment of the nonhydrogenic Stark effect, the problem of dealing with closed channels never arises since all channels are asymptotically open in the presence of the electric field. The present paper has not faced this problem either, although it is much more relevant here in the context of negative-ion photodetachment in a magnetic field. In fact, whenever the binding energy of a zero-field resonance becomes comparable to

the Landau-level spacing, the preceding theoretical development has questionable validity. Even the application to Rb^- photodetachment shown in Fig. 6 has somewhat borderline validity for a 10.7-kG magnetic field. It seems plausible to expect that the local spherical-cylindrical frame transformation can be suitably generalized to incorporate this essential physical element, but this task will be left to subsequent investigations. Related difficulties are discussed for the Stark field treated in Ref. 7. In any case, the present approach should provide a correct description of nonresonant photodetachment in a magnetic field, and of resonant photodetachment in the vicinity of resonance structures which are much broader in zero-field than the Landau-level spacing.

ACKNOWLEDGMENTS

I am indebted to D. Harmin and C. W. Clark for discussions in the early stages of this work. Some of the results of Sec. II C, including Eqs. (22) and (27), in particular, were independently derived by D. Harmin. This work was supported in part by the National Science Foundation, and in part by the Alfred P. Sloan Foundation.

[1]W. A. M. Blumberg, R. M. Jopson, and D. J. Larson, Phys. Rev. Lett. **40**, 1320 (1978).

[2]W. A. M. Blumberg, W. M. Itano, and D. J. Larson, Phys. Rev. A **19**, 139 (1979). This work derives a theoretical description which seems largely equivalent to that of G. G. Pavlov, Opt. Spectrosk. **33**, 1006 (1972) [Opt. Spectrosc. (USSR) **33**, 554 (1972)].

[3]C. W. Clark, Phys. Rev. A **28**, 83 (1983).

[4]A. R. P. Rau and U. Fano, Phys. Rev. A **4**, 1751 (1971).

[5]D. Harmin, Phys. Rev. Lett. **49**, 128 (1982); Phys. Rev. A **26**, 2656 (1982); Comments At. Mol. Phys. **15**, 281 (1985).

[6]U. Fano, Phys. Rev. A **24**, 619 (1981).

[7]Hin-Yiu Wong, A. R. P. Rau, and C. H. Greene (unpublished).

[8]For recent reviews, see C. W. Clark, K. T. Lu, and A. F. Starace, in *Progress in Atomic Spectroscopy, Part C,* edited by H. J. Byer and H. Kleinpoppen (Plenum, New York 1984), p. 247; M. R. C. McDowell and M. Zarcone, Adv. At. Mol. Phys. **21**, 255 (1985).

[9]C. M. Lee, Phys. Rev. A **11**, 1692 (1975).

[10]U. Fano and A. R. P. Rau, *Atomic Collisions and Spectra* (Academic, Orlando, 1986).

[11]C. H. Greene, A. R. P. Rau, and U. Fano, Phys. Rev. A **26**, 2441 (1982); **30**, 3321 (1984); C. H. Greene, U. Fano, and G. Strinati, *ibid.* **19**, 1485 (1979).

[12]See, for instance, I. I. Sobel'man, *Introduction to the Theory of Atomic Spectra* (Pergamon, New York, 1972), Chap. 4.

[13]C. H. Greene and Ch. Jungen, Adv. At. Mol. Phys. **21**, 51 (1985).

[14]C. H. Greene, Phys. Rev. A **22**, 149 (1980).

[15]I. S. Gradshteyn and I. M. Ryzhik, *Table of Integrals, Series, and Products,* 4th ed. (Academic, New York, 1965), Eqs. (7.333.1) and (7.333.2).

[16]*Handbook of Mathematical Functions,* edited by M. Abramowitz and I. A. Stegun (Dover, New York, 1965), p. 775.

[17]D. J. Larson and R. Stoneman, Phys. Rev. A **31**, 2210 (1985).

[18]O. H. Crawford, Bull. Am. Phys. Soc. **30**, 856 (1985).

[19]S. Watanabe and C. H. Greene, Phys. Rev. A **22**, 158 (1980).

[20]N. Rouze and R. Geballe, Phys. Rev. A **27**, 3071 (1983).

[21]P. Frey, M. Lawen, F. Breyer, H. Klar, and H. Hotop, Z. Phys. A **304**, 155 (1982).